6-th International TEPA Symposium
Thunderstorms and Elementary Particle Acceleration
October 3-7| Nor Amberd| Aragasotn Province| Armenia
2016

Physical analysis of multivariate measurements in the Atmospheric high-energy physics experiments within ADEI platform

K.Avakyan[1], S.Chilingaryan[1,2], A.Chilingarian[1], T.Karapetyan[1]

1. A.Alikhanyan National Lab (Yerevan Physics Institute), 2 Alikhanyan Brothers, Yerevan 0036, Armenia,
2. Karlsuhe Institute of Technology, Germany

Abstract. To make transformational scientific progress in Space science and geophysics, the Sun, heliosphere, magnetosphere and different layers of the atmosphere must be studied as a coupled system. Presented paper describes how information on complicated physical processes on Sun, in the heliosphere, magnetosphere and atmosphere can be made immediately assessable for researchers via advanced multivariate visualization system with simple statistical analysis package. Research of the high-energy phenomena in the atmosphere and the atmospheric discharges is of special importance. The relationship between thundercloud electrification, lightning activity, wideband radio emission and particle fluxes have not been yet unambiguously established. One of most intriguing opportunities opening by observation of the high-energy processes in the atmosphere is their relation to lightning initiation. Investigations of the accelerated structures in the geospace plasmas can as well shed light on particle acceleration up to much higher energies in the similar structures of space plasmas in the distant objects of the Universe.

1. INTRODUCTION

In recent years, the interest in using cosmic rays for obtaining information on atmospheric and extra-atmospheric processes is rapidly growing. Cosmic rays are modulated by the solar bursts and can be used as messengers carrying information on upcoming space storms. Precise and continuous monitoring of the secondary cosmic rays with networks of particle detectors can reveal the danger of agents of solar activity (Interplanetary coronal mass ejections and solar energetic proton events). Appropriate scientific infrastructure and analysis methodology was developed at the Cosmic Ray Division (CRD) and tested on the violent events of the 23-rd solar activity cycle (1997-2008, Chilingarian, 2009, Bostanjyaa n and Chilingarian, 2009, Chilingarian and Bostanjyan, 2010, Mailyan and Chilingarian 2010, Hovhannisyan and Chilingarian, 2011, Chilingarian and Karapetyan, 2011). Recently it was discovered that fluxes of cosmic rays detected on the earth's surface also carry information on the parameters of atmosphere, primarily on very difficult to measure atmospheric electricity (Chilingarian et al., 2010, 2011, 2012a). Fluxes of gamma rays and electrons carry information on high-energy processes in the atmosphere and on the net potential of atmospheric electric fields associated with emerging positive and negative charged layers in thunderclouds. Fluxes of the "thunderstorm" neutrons, first reliably detected on Aragats (Chilingarian et al., 2012b and 2012c) are connected with the photonuclear reactions of the gamma rays with atmospheric nuclei and can pose radioactive hazard to crew and passengers of the nearby aircrafts (Drozdov et al., 2012). The muon flux provides the main contribution to the natural ionizing radiation at the Earth's surface. Cosmic ray muons come to the observation point from all directions of the upper celestial hemisphere and are sensitive to any changes in the flux of primary cosmic rays and the meteorological conditions high in the atmosphere. A comprehensive study of all aspects of the impact of atmospheric and extra-atmospheric processes on cosmic rays require as many measurements of various components of cosmic rays as possible.

One of the recognized leaders in contemporary investigations of geophysical phenomena using cosmic ray is the Cosmic Ray Division (CRD) of the A.Alikhanyan National Scientific Laboratory of Armenia and its Aragats Solar Environmental Center (ASEC). At CRD's Aragats and Nor Amberd research stations the networks of detectors registering electrons, muons, gamma rays and neutrons operate round the clock, providing important information on various geophysical processes. Methods for visualization and analysis of multi-dimensional experimental data developed in the laboratory are successfully used to research solar-terrestrial connections and high-energy phenomena in the terrestrial atmosphere. Modern devices to measure magnetic and electrical fields, meteorological conditions, and lightning occurrences were placed at the Aragats and Nor Amberd research stations. Data from this instrumentation and the associated research gave us important information about the fluxes of electrons and gamma rays from thunderclouds. Detected particles and the penetrating radiation from thunderclouds give information on the local changes of the electric field and other key metrological parameters. Multivariate analysis of variations of fields, radiation, and particle fluxes can provide new information on the development of thunderstorm anomalies in the atmosphere, including those of catastrophic nature. Such analysis presents a challenge due to the large quantity of acquired data. Huge amount of time series should be processed and identified near on-line for forecasting and alerts, as well as for report and paper preparation. Usually, researchers have no time to access archives if the data stream is pressing and new interesting events appear each new day. Therefore, to support researcher in data mining and finding "new physics" a multivariate visualization platform should be supplemented with tools of elementary statistical analysis (histograms, moments, correlations, comparisons); figure preparation; archiving, i.e. with a data exploration system.

Therefore, we supply the online stream of "big" data from ASEC with an exploration system developed in a collaboration between Karlsruhe Institute of Technology (KIT). The Advanced Data Extraction Infrastructure (ADEI, Chilingaryan et al., 2010) helps researchers in exploring and understanding solar-terrestrial connections, solar modulation effects as well as in understanding high-energy phenomena in the atmosphere. A user-friendly interface interactively

visualizes the multiple time-series and selects relevant parameters for different research objectives. Time series from different domains are joining for a multivariate correlation analysis. The developed software links a multitude of space and geophysical observations into an integrated system and provides analysis tools and services to fully utilize the scientific potential of current space weather/geophysical observations. In this way, we try to fully utilize the new concept of "big" data when an enormous amount of relevant observations culminates in the "new" physics unprecedentedly fast and precise. In this paper, we will focus on the new options of the ADEI that allows not only on-line displaying the multivariate measurements, but also on-line analyze the physical phenomena.

2. ADVANCED DATA EXTRACTION INFRASTRUCTURE (ADEI)

ADEI (Chilingaryan et al., 2010) has been developed to provide data exploration capabilities to a broad range of physical experiments dealing with time series.

All these systems have very different characteristics: an amount of data channels, their types, sampling rates, etc. The data is stored in many different ways utilizing various data formats and underlying database engines. On the other side, users need information in different data formats, which are supported by analysis tools they use for post processing. Besides, operators need a tool providing possibility to examine all collected data checking the integrity and validity of measurements. It is also needed to search and export data possessing specified characteristics.

To provide such a broad coverage ADEI utilizes highly modular architecture. The system consists of backend and frontend parts communicating over HTTP protocol using Asynchronous JavaScript and XML (AJAX, see for references to software used Chilingaryan et al., 2010) approach. The ADEI backend defines few abstract interfaces which are used to implement various capabilities using simple plugins. The data sources are interfaced with dedicated drivers implemented data access abstraction layer. The higher levels of the system are utilizing this abstract interface to get data in a uniform way from arbitrary storage.

The ADEI web frontend is inspired by GoogleMaps interface. Single or multiple time series are plotted using the data from currently selected time interval. Then, the plot could be dragged and zoomed over time and investigated parameters value. The desired region of the plotted variables may be selected for detailed statistical analysis or exported in one of the supported formats.

2.1. ARCHITECTURE

ADEI is designed to deal with the data sampled at high rates and stored for long periods of time. The time span of measurements at ASEC goes back for 20 years and the fastest detectors are sampling the data at rates exceeding 10 Hz. Processing such amounts of data requires enormous computational power. However, the interactive tools should operate in near real-time and extract important information from this enormous amount of data. To achieve this goal ADEI continuously monitors incoming data, performs preprocessing, and caches important information in a high performance database.

The simplified diagram of ADEI architecture is presented on Figure 1. The main logic of ADEI system is contained in a backend which is implemented purely in PHP programming language. The backend incorporates a data access layer, a caching daemon, an ADEI library. Communication with the web frontend and other client applications is maintained using web services. HTTP protocol is used for data exchange, XML for data encoding.

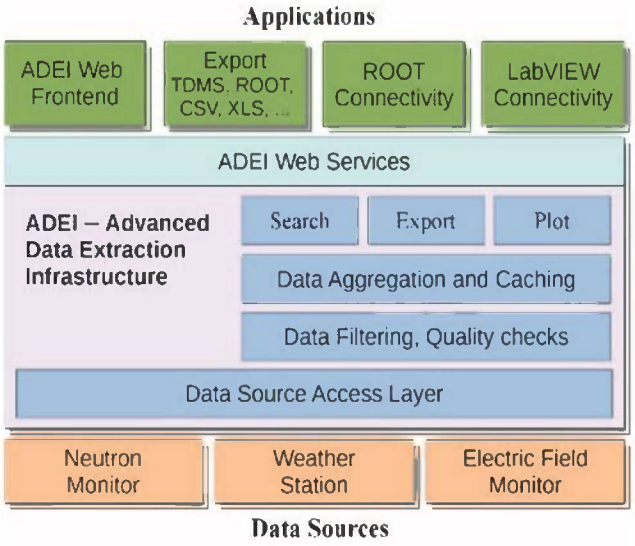

Figure 1. Architecture of Advanced Data Extraction Infrastructure. Data Source Access Layer unifies access to the time series stored in different formats. After data filtering and quality checks the data is aggregated and stored in intermediate caching database. Access to the data is provided by ADEI library and web services are used to communicate with client applications.

The data access layer hides details of underlying data sources providing other components of the system with a uniform way of data access. The data is organized hierarchically. The top level of hierarchy is the data source and ADEI may underline several data sources. The time series provided by the data source is divided in time-synchronized groups, so called *LogGroups*. The current version includes modules to access data stored in relational databases accessible through PDO or ODBC interfaces, several NOSQL databases, RRD (Round Robin Database Tool) data format used by many system monitoring applications. Most of popular databases including MySQL/MariaDB, PostgreSQL, Oracle, Microsoft SQL server, and CoucheDB are supported.

The caching daemon is continuously running on a backend server and polls all data sources for a new data. When the data is acquired it piped through series of filters which check the data quality, apply correction coefficients and drop invalid data. Then, the data is aggregated over intervals of few different periods. For each period, called *cache level*, statistical information is gathered and stored in MySQL database (*caching database*) as additional time series. Minimum, maximum, and arvergage values, the total number of recorded records, and the amount of invalid or missing records for each interval of aggregation are stored. Then, this caches are used by ADEI to speed-up searches or provide data averaged over the specified intervals. For instance, the plot module first selects the maximal cache level providing enough points to generate the plot of the specified size. The time resolutions of caching database are selected in the way that between 1000 and 10000 data samples can be extracted for any specified interval. Such an amount of points fulfills most of plotting demands and in the same time the plots could be generated relatively fast. After

selection of cache level is made, the data is extracted from correspondent caching tables and one of supported algorithms is used to convert aggregated values into the graphic points. The data plots are generated with JpGraph on the backend and delivered to frontend as PNG images.

ADEI provides the stored data in multiple formats. We currently support CSV (Comma Separated Values), Microsoft Excel, NetCDF, ROOT (an analysis framework for high energy physics), and TDMS (Technical Data Management Streaming). Additional formats may be implemented in two ways. The ADEI supports custom export plugins. Alternatively, it is possible to filter exported data using system scripts. For example, to generate ROOT output, the data in CSV format is piped to standard input of a simple ROOT application which converts it to ROOT format and prints to standard output. The same mechanism could be used to compress output before returning it to the client application. The chains of filters are supported. This allows to produce archived ROOT files. To limit amount of the exported data, a resampling by averanging or summing up can be requested.

ADEI search engine is implemented with pluggable search modules and is able to search for channels, channel groups, channel values, and time intervals. The channel search is very flexible. The channel names and descriptions are searched for single and multiple words, exact phrases, and regular expressions. The words are matched in three different ways: exact match, words starting with the search term, or words containing search term. The search is case-insensitive and all types of matching can be mixed in a single query. The value search finds a set of time intervals where the values of the given channel are above/below the specified threshold. The two modes are supported: search for time intervals where any value from the interval is above/below the specified threshold and search for time intervals where at least some of the values are above/below the threshold. The data cache is used to accelerate searches over big amounts of data and all searches are executed within few hundred milliseconds. The interval search allows users to quickly position time axes. The search module supports strings like January 2005 or January - March, 2006 and upon submitting of search request the time axis will be set accordingly.

Meteorological information is represented by time series of measurements of automatic weather stations and photograths of lightning discharges in the sky. Though it is impossible to process photographs using standard data aggregation chains in ADEI, we built a "Custom" data chain to provide a uniform access to the images using standard interfaces with minimal restrictions. The data source may optionally provide, so called Custom data, where each data channel is associated with custom array instead of scalar. The module handling the data from relational databases provides such Custom channels from the binary BLOB data stored in the database. As caching for images is currently not available, the visualization modules requests data directly from the database. This limits applicability to rather small time intervals, but allows us to provide additional information in ADEI web interface while analyzing specific atmospheric events. As well, ADEI filtering subsystem is able to creatie derivative data channels based on the filter output. It allows us to feed images into the chain of filters and extract scalar values characterizing some properties of the recorded data. For example, from the lightning discharges picturewe can extract number and lentgh of lightning and make it available to the scientists via ADEI.

2.2. FRONTED

The main view of ADEI web frontend is represented on Figure 2 and the numeric labels from 1 to 12 are used to reference interface elements in the description below. The main window (label 1) contains plot depicting measurements of 7 sensors on a voltage, temperature, and default axes.

The channel to axis mapping can be defined either by the source database or in the ADEI configuration. All unmapped channels are displayed using optional default axes. There is no hard limit on a number of supported axes, but rather the size of the browser window is only factor restricting the number of axes which can be reasonably displayed.

The data for period of approximately two weeks is shown. During this period, the registrations of sensors were sampled into the database approximately ten times in a second what gives about 12 millions of data records over two week interval. For visualization, this data is aggregated and approximately a few thousand data points are extracted from the caching database to render the graph. The system is optimized in a way that complete time of rendering does not exceed a few hundred milliseconds on a standard desktop hardware. Sometimes, however, the collected information includes periods when no data was recorded or existing recordings are invalid. Due to aggregation, the short outtages is impossible to see on the low zoom levels. In order to handle such situations, ADEI includes a quality indication line on a top of the data plot (just below a plot title). On the screenshot it is possible to see a tiny line indicating short period when the data was not recorded due to power outtage (see label 5).

The ADEI is configured using various controls in the sidebar. The lower part (label 7) allows to set various options controlling behavior of export subsystem, data aggregation and visualization modes, etc. The top part (label 6) includes 3 tabs controlling which data is displayed on the plot. The Source tab allow to select one of the pre-configured groups of channels. More flexibility can be achieved with Source Tree tab of the bottom sidebar (label 7) which allows to select individual channels from the hierarchical tree. The Axes tab allows to tune the axes by specifying their ranges and switching between standard and logarithmic modes. Time tab is used to configure the time interval of interst. Few different modes are supported. The data source may provide a list of time intervals when something important was happening. It is possible to select a desired interval from this list and apply it to the time axis. Alternatively, the beginning and the end of time axis could be set manually with a microsecond precision. Other options include visualization of all stored data or just last quantity of seconds (i.e. plot for last minute, hour, day, week, etc.). In the last case the plot will be periodically updated to display incoming data.

It is also possible to zoom into the regions of interest on the plot using mouse. The subarea of plot can be selected using mouse pointer while holding left button (label 2). After selection is made it still can be fine tuned: resized or positioned using mouse or keyboard arrows. The buttons in the right-bottom part are used to export data within selected time interval (label 3) or to zoom into the selection (label 4). Additional functional buttons can be implemented using custom plugins. Also, the current plot on display can be zoomed in and out by scrolling mouse wheel. The default

action is to zoom along time axis at the position of mouse pointer. However, the key modifiers may be used to zoom over value axis or zoom in the center of the plot. The adjustments of plot position on the time and value axes are achievable by scrolling mouse over the correspondent axis. The double click on considered axis will restore it into the automatic mode and the general overview will be displayed again. Finally, the ADEI supports navigation history. Forward and Back buttons of the browser could be used to go back and forth in the history. The URL in the navigation bar is always precisely describing current position, selected time series, and all configured properties. This URL could be sent to the colleagues over e-mail and exactly the same plot will be displayed on their PC.

A status bar (label 10) is used to provide status and contextual messages to the user. Currently performed actions, their completion status, contextual help, emerging error messages are reported using status bar. On mouse movement the position of mouse pointer along all axes is reported as well. An example could be seen on the provided screenshot. The color coding is used to help with association of axes. ADEI also provides possibility to investigate graphics passing in the specified area of the plot. A legend window (label 10) is popped up when the left mouse button is clicked. It contains a list of all graphics on the plot which are passing near position where mouse was clicked. The short name, description, and a range of values possessed in the neighborhood are presented on the legend.

ADEI provides advanced search and simple integrated WiKi engine. Upon entering a search string (label 11), the bottom sidebar (label 7) is opened and results are reported in the Search tab. The example on screenshot displays results of searching for temperature sensors. The WiKi engine is normally used to describe the data channels available in the system and provides several specific extensions on top of standard WiKi syntax. [preview] - generates a preview plot. The channel group, time interval, image size, aggregation mode, and other standard properties may be specified. The preview is linked and upon a click will switch to the plotting view and display appropriate graph. [grouplist] - generates linked previews for all channel groups available in the system. [channels_by_name] - includes alphabetical listing of all channels in the system. Upon a click the selected channel will be plotted. [channels_by_group] - includes hierarchical listing of all channels in the system. The selected channel will be plotted upon a click as well. The example Wiki pages are depicted on Figurues 3 and 4.

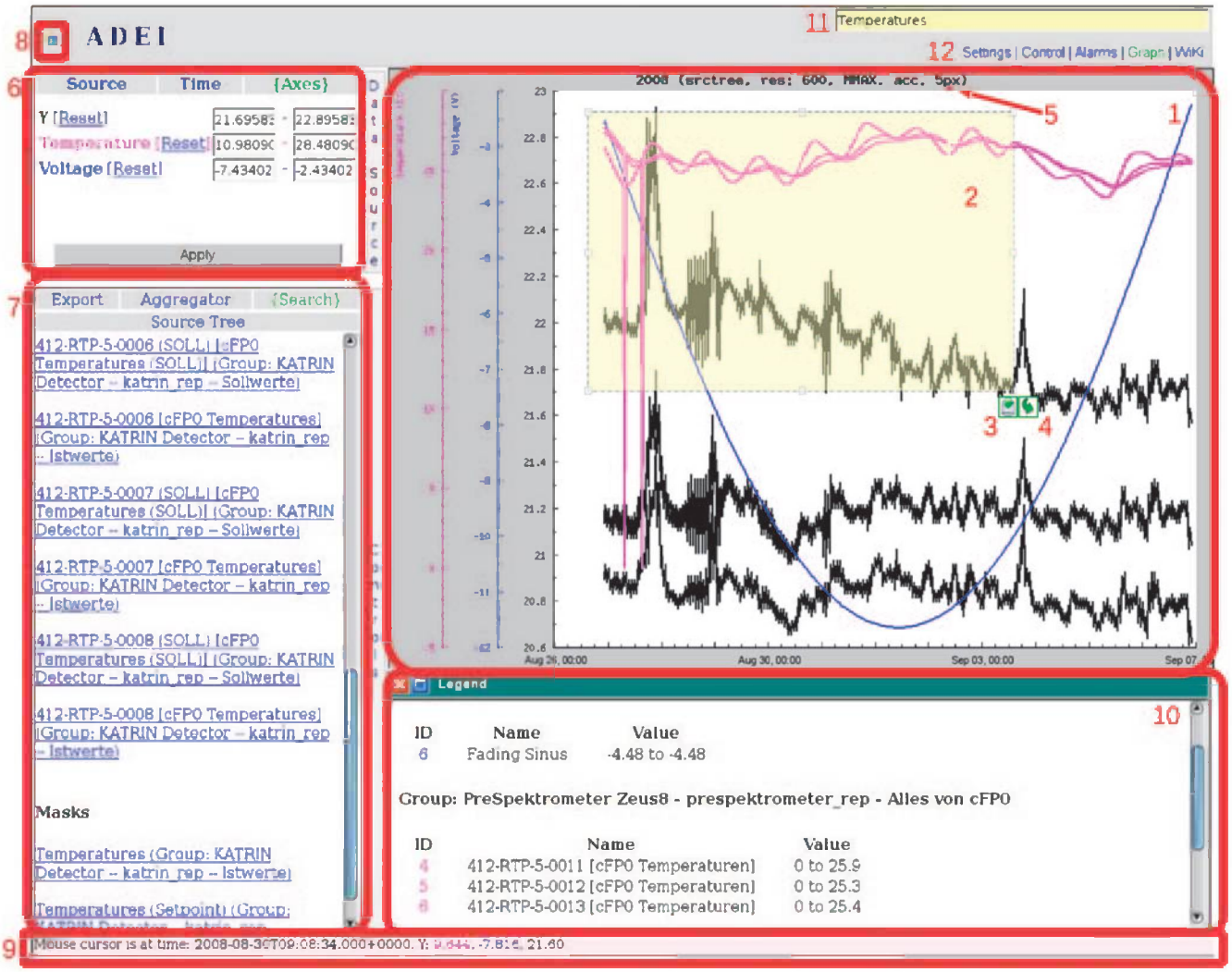

Figure 2. Screenshot of ADEI Web Frontend. The data outage is indicated using a small line on top of the plot (see 5). Legend contains description of displayed graphics. The selected part of plot may be zoomed or exported using buttons 3 and 4. Axes controls and results of search are located in the left sidebar.

Advanced Data Extraction Infrastructure of Aragats Space Environmental Center (ADEI of ASEC)

Dear user, welcome to the ASEC Advanced Data Extraction Infrastructure! The ASEC ADEI is loaded and ready to work.
Please select the data ***Source*** and ***Time*** interval from the ***Data Source*** popup on the left sidebar, or use the pulldown menu in the top-left corner.

Navigation through the data done with the mouse:

- Drag with left mouse button to select a region.
- Click on the arrow button to zoom inside a region.
- Use the mouse wheel shift current window left and right.

To **download** selected data open choose the ***Export*** tab from ***Controls*** popup. You can export data to the multiple supported formats. Please be patient, as exporting data may take a while.

More detailed information about how to use ADEI can be found in the **ADEI Users' Guide**. To find more information about ADEI system and report bugs, please, visit project home page. Please read this publication to get more information how is working ADEI.

The Efficiencies of the ASEC particle detectors used in Thunderstorm Ground Enhancement (TGE) research (Bagrat Mailyan)

Below you will find **descriptions of the monitors** and their data.

Aragats Research Station (40.47N, 44.18E, 3200m a.s.l.)
AMMM - Aragats Multichannel Muon Monitor
ArNM - Aragats Neutron Monitor
ASNT - Aragats Solar Neutron Telescope
Cube - Neutral Cosmic Ray Monitor
MAKET - MAKET-ANI Extensive Air Shower Detector
NaI - NaI(Tl) Monitor
SEVAN - SEVAN Monitor at Aragats
Stand_1cm - Plastic Scintillator Monitor for Low Energy Particles
Stand_3cm - Plastic Scintillator Monitor with Spectral Analysis
Electric Field - Electric Field Monitor at Aragats
Lightning Detector - Lightning Detector at Aragats
LEMI-417 - Magnetotelluric Station (MTS)
Weather Station - Davis Wireless Vantage Pro2 Plus

Yerevan CRD headquarters (40.205N, 44.486E, 1090m a.s.l.)
SEVAN - SEVAN Monitor at Yerevan
Electric Field - Electric Field Monitor at Nor-Amberd
Lightning Detector - Lightning Detector at Nor-Amberd
Cube_3cm - Magnetotelluric Station (MTS)
Weather Station - Davis Wireless Vantage Pro2 Plus

Sevan Lake (40.619N, 45.028E, 1910m a.s.l.)
Stand_1cm - Plastic Scintillator Monitor for Low Energy Particles
Electric Field - Electric Field Monitor at Nor-Amberd
Lightning Detector - Lightning Detector at Nor-Amberd

SEVAN Monitors
SEVAN Aragats - SEVAN Monitor at Aragats
SEVAN Nor-Amberd - SEVAN Monitor at Nor-Amberd

Figure 3. Screenshot of ADEI Wiki page (left part of the screen). Thelist of ASEC detectors and links on the pages with detailed detector description.

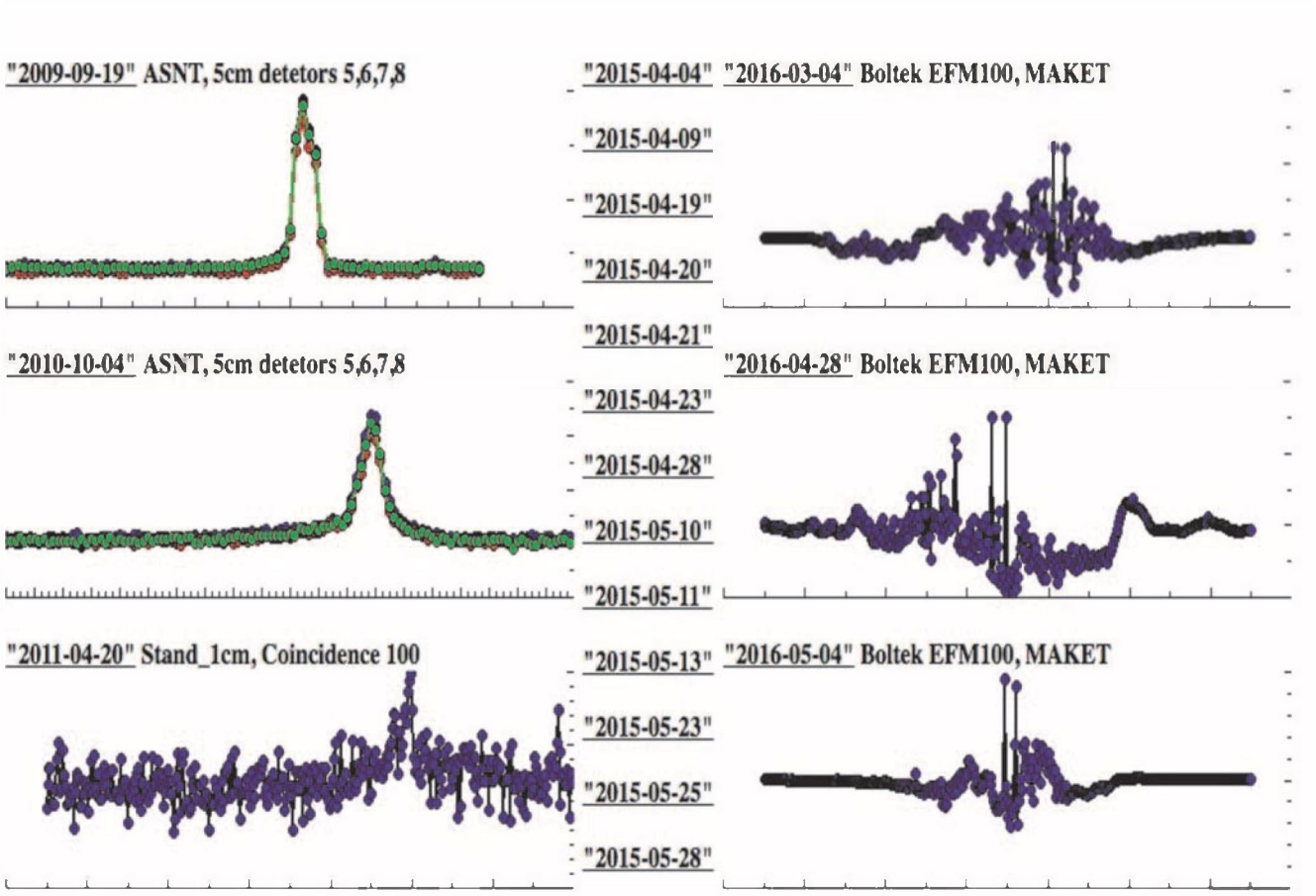

Figure 4. Screenshot of ADEI Wiki page (right part of the screen). Previews of most interesting events (event katalog). By clicking on the preview, the appropriate analysis session for the selected event will be opened in the main ADEI screen.

2.3. ADEI SECONDARY MODULES (PANELS)

More inforamation in textual and visual forms may be provided in ADEI using so called secondary views. The secondary views are implemented with plugins which get all information about current ADEI screen on the display and all configured options. Based on thsese information, the relevant information is requested from ADEI backend and presented to the user in variety of forms. If necessary the views may interact with users by adding additional forms in the generated HTML content.

A set of secondary modules is available for ADEI to extract statistical information from the time series and provide basic insight in cross-correlations between different channels. The particle detectors at ASEC measure modulation of the stable galactic cosmic ray "background" by solar and local weather phenomena. Therefore, ADEI is often used to find a peak in a noisy random environment. A "background" module is a core component of the analysis platform. Using ADEI standard display, it allows the user to select an interval before an interesting event happened (for instance a particle flux from thunderclouds originated large peak in the time series) and extract the required statistics from it. For each of the data channels in ADEI, the module provides standard statistical information about the selected background to the users and other ADEI modules. For instance, the mean value and standard deviation on fair weather. Using calculated values it will be possible to show the time series in percent to the "background" value or in the number of standard deviations from the mean value. These options allow comparing and correlating variables with significantly different mean values on the one and the same frame. To verify correctness, additionally, the module shows a histogram and applies a Gaussian fit to the count rate histograms.

There are as well other secondary ADEI modules, which provide statistical information on the data, which is on display in the main ADEI window. First of all, for each channel the "channel list" module reports minimum, maximum, average and standard deviation of measurements in the selected interval as well as the minimum and maximum in the units of percent and standard deviation. For optimal performance, for larger time intervals an estimated value of standard deviation is computed using the averages from the ADEI cache. The "histogram" module show the histogram of the selected channel currently on display. The module supports normalization of the histogram and allows the user to perform Gaussian fit of the displayed data. In the upper right corner of the plot, the user sees the mean value of a variable in the selected data interval, the standard deviation, and Pearson`s chi-square test value. The number of bins is configured automatically or may be specified by the user.

The "scatter plot" module is for visualization of the relation of 2 variables. The linear correlation coefficient of the selected pair of variables is calculated and depicted on the plot as well. Delays between signals registered by different detectors can be found out using the "correlation plot" module. It allows viewing the dependence of the correlation coefficient depending on the added delay of one of time variables related to the second one. The user is expected to specify a step in the seconds, minutes, hours, or days.

3. USING ADEI FOR DATA MINING AND PHYSICAL ANALYSIS

Experiments in the field of the atmospheric high-energy physics produce the continuous high-volume stream of data from monitoring of neutral and charged particle fluxes, from high-speed cameras, field meters and lightning mapping arrays. Gaining in- sights from enormous volumes of such diversity of observations poses a number of challenges to data analysis chain and physical inference techniques.

The adopted method of the multivariate data analysis and physical inference consists in the selection of the hierarchical time series of particle count rates along with measurements of the electric field, distance to lightning, fast electric field waveforms and other. Precise synchronization of all measurements allows analyzing the time series on millisecond time scales. The one-second and one-minute time series also are very useful for discovering many non-trivial correlations in TGE data. Analyzing numerous TGEs registered on Aragats with one and the same sequence of patterns we reveal the repeating structures, typical correlations and finally causal relations between observables. As a result, we come to models and theories of TGE initiation and its relation to the electrical structure of the thunderclouds and lightning initiation and propagation. Multivariate analysis methodology becomes possible only with the use of ADEI - a very flexible and powerful tool providing services for the multidimensional visualization, interactive decision support, data zooming, comparison, digitizing, statistic analysis and other. We demonstrate how instrumental is the ADEI platform in physical inference taking as an example analysis of one of most intensive TGEs measured by facilities of the ASEC.

We illustrate ADEI procedures implementing visualization/analysis methods to TGE occurred on 16 June 2016 (Fig 5). First considered frame contains exhausted information on the storm, including time series of electrostatic field disturbances, the 1-minute count rate of the particle flux, solar radiation, rain rate and distances to lightning flashes. Storm started ~ 7:30 UT and continued until 11:30. All this time electrostatic field significantly differs from the fair weather value of ~ 140 V/m. At the deeps of negative field we see enhancements of count rate measured by 1-cm thick outdoors plastic scintillator with energy threshold to measure charged particles ~ 1 MeV. The deepest negative field of -21.5 kV/m coincides with largest peak in particle detector count rate. The solar energy decreased from ~500 W/m2 down to less than 100 W/m2 due to thundercloud screening earth's surface from sun. No rain was detected, thus the charges were not washed out from the cloud and separated differently charged layers in the cloud continuously induce significant electric field and potential drop. Nearby lightning flashes influence electric field and particle flux; these effects will be investigated with more detailed frames later.

Thus, the start of TGE event analysis started from the frame shown in Figure 7. We see how the thundercloud is reaching the skies above detectors location site; how the particle flux start to rise and how it was terminated by lightning.

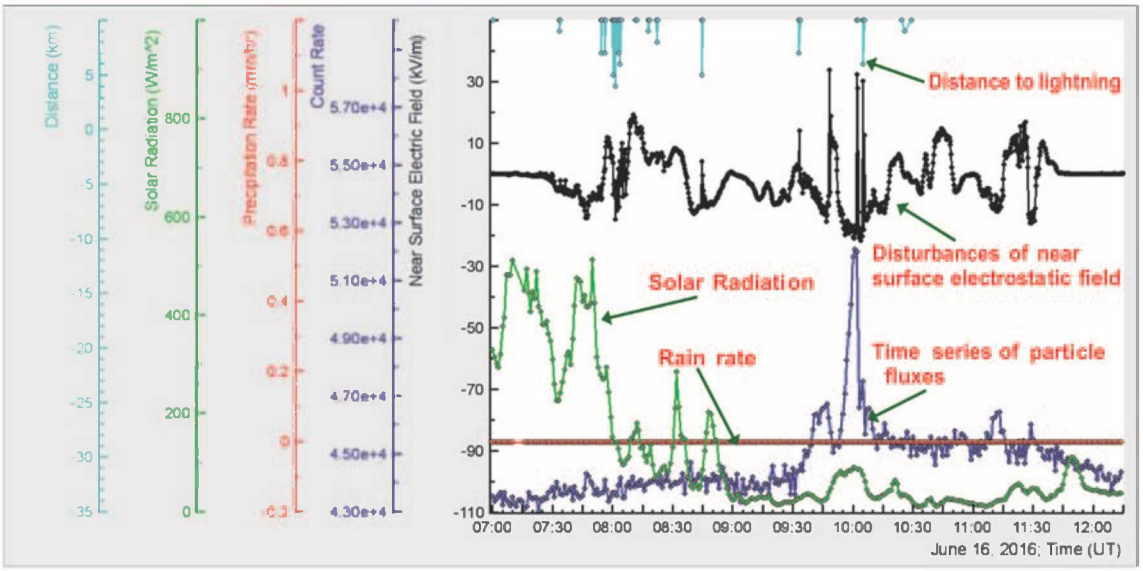

Figure 5. Meteorological and radiation information on the severe storm on Aragats.

Analysis of the next frame gives us more information on particle fluxes (Figure 6). In Figure 6c we show time series of, so called, coincidences or combinations of particle detector STAND3 comprised from stacked vertically 3-cm thick plastic scintillators. Data acquisition electronics of particle detectors provide not only counting of a number of particles hitting each scintillator, but also – coincidences of "firing" of different detector channels. For instance "1000" combination corresponds to the signal only in the upper scintillator i.e. low energy particle (less than 4-5 MeV) stopping in the 3 cm of plastic in the first scintillator. Following coincidences select particles of higher energies. The pattern of all coincidences shown in Figure 6c gives information on TGE energy spectra. The count rate is shown not in the absolute rates, but in the number of standard deviations. First of all, only in this way we can compare time series with drastically different mean values. Moreover, in this way we can estimate the statistical significance of detected peaks and compare different TGEs by, so called, σ criteria. The largest peak, as we can see in Figure 6c is ~ 20 σ. Certainly, we cannot calculate the chance probability (probability that peak is a fluctuation of the Gaussian population only) for such a gigantic significance; values of the σ criteria will be used for comparative purposes only. The type of count rate presentation is selected from the special menu located in the left side of ADEI layout.

Analysis of the next frame gives us more information on particle fluxes (Figure 6). In Figure 6c we show time series of, so called, coincidences or combinations of particle detector STAND3 comprised from stacked vertically 3-cm thick plastic scintillators. Data acquisition electronics of particle detectors provide not only counting of a number of particles hitting each scintillator, but also – coincidences of "firing" of different detector channels. For instance "1000" combination corresponds to the signal only in the upper scintillator i.e. low energy particle (less than 4-5 MeV) stopping in the 3 cm of plastic in the first scintillator. Following coincidences select particles of higher energies. The pattern of all coincidences shown in Figure 6c gives information on TGE energy spectra. The count rate is shown not in the absolute rates, but in the number of standard deviations. First of all, only in this way we can compare time series with drastically different mean values. Moreover, in this way we can estimate the statistical significance of detected peaks and compare different TGEs by, so called, σ criteria. The largest peak, as we can see in Figure 6c is ~ 20 σ. Certainly, we cannot calculate the chance probability (probability that peak is a fluctuation of the Gaussian population only) for such a gigantic significance; values of the σ criteria will be used for comparative purposes only. The type of count rate presentation is selected from the special menu located in the left side of ADEI layout.

The "scatter plot" option is selected from statistical analysis menu that appears at the left side of the ADEI layout. In the inserts, we show scatter plots revealing the interrelation of selected variables. The scatter plot 6a showing large positive correlation is rather trivial: high-energy particles after hitting upper scintillator are hitting and registering by other scintillators located just below and, certainly, correlation should be positive. The scatter plot 6b revealing the negative correlation between 1111 and 1100 combinations is a somewhat surprising, illuminating interesting physical phenomenon. Due to the dominant positive charge of galactic cosmic rays, the positive muons are prevailing the negative ones. This important for many physical applications effect is evident for the muons with energies below 100 MeV; the increase can reach ~10% and more. Most of the particles counted as "1111" coincidence are muons (both positive and negative, we can not distinguish them); the probability that gamma ray is responsible for such a combination is ~10-7 and there can be only very few electrons with energies above 20-25 MeV reaching surface detectors from the thundercloud. Thus, during TGE the electric field in thundercloud that accelerates and multiplies electrons will decelerate the positive muons diminishing the count rate of 1111 combination. The 1100 combination during TGE will certainly enhance. Thus, we explain the negative correlation and, moreover, we can pose interesting physical problem acquiring data from the Figure 6. We can try to estimate the electric field strength that accelerates electrons and stop the positive muons. And we can try to estimate the charge ratio of cosmic ray muons. Both problems are very important for the atmospheric and cosmic ray physics.

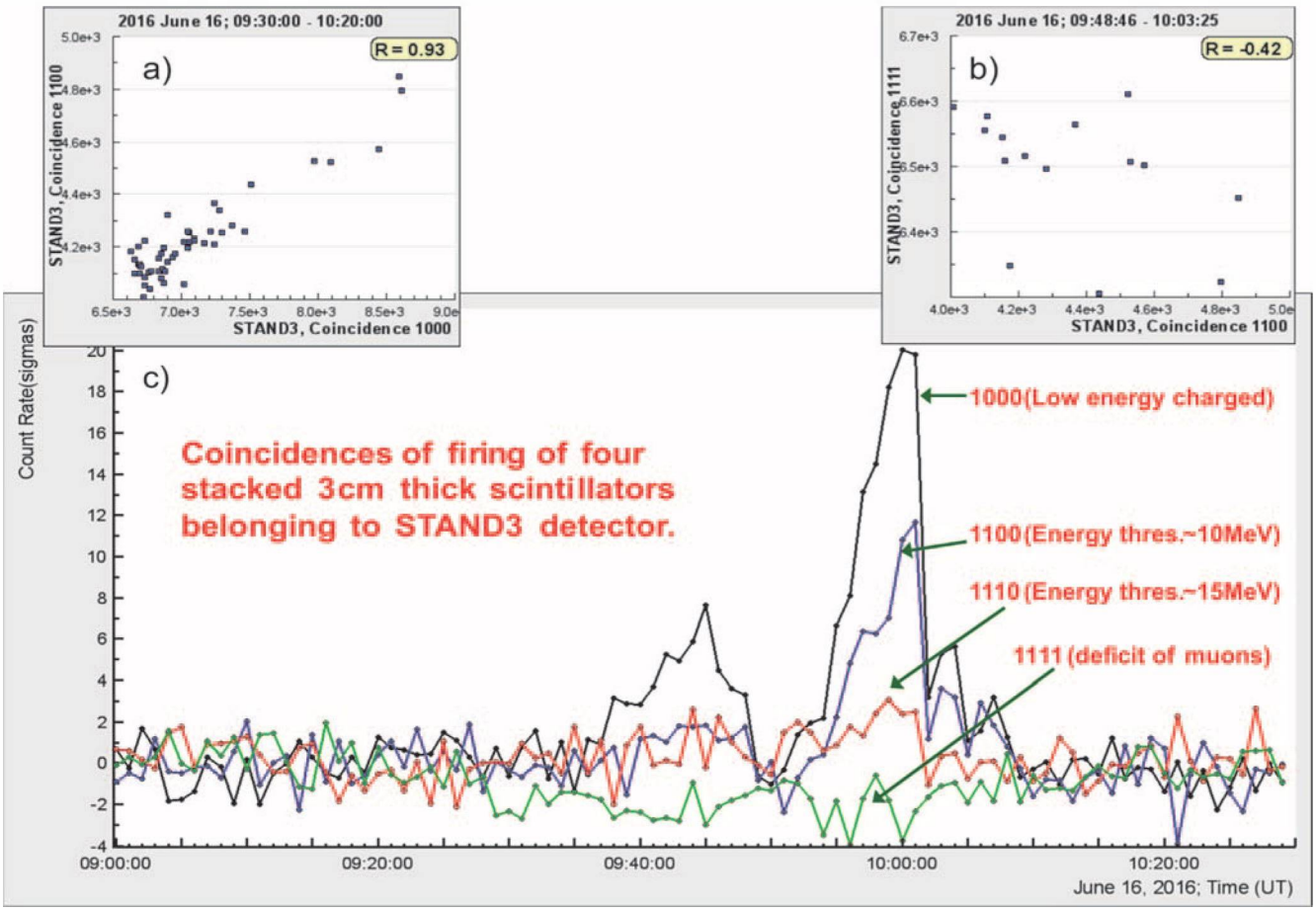

Figure 6.. Time series of STAND3 detecor coincidences in the "number of standard deviation" scale. Rough estimate of energy spectra. In the incert we demonstrate correlation analysis of the STAND3 detector coincidences.

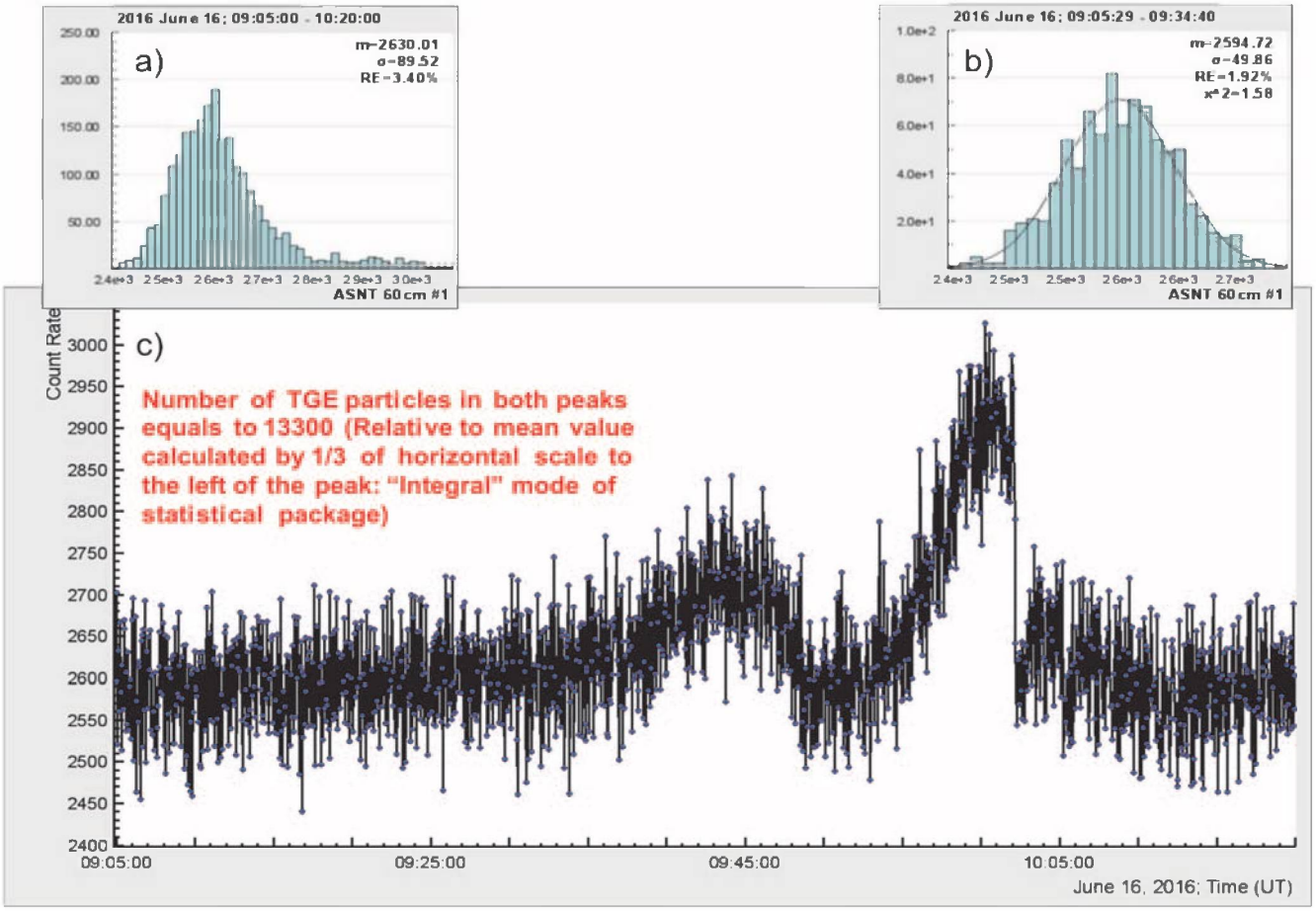

Figure 7. Enumeration of number of additional (relative to mean) particles detected during TGE. In insert histograms of count rates of 60 cm thick plastic scintillator of whole and one third of horisontale scale are shown.

Another statistical procedure is "Histogram". In Fig 7a we show the histogram of count rates of the 60 cm thick plastic scintillator of ASNT detector shown below in the Figure 7c. Due to peaks in time series (TGEs) histogram significantly diverges from the Gaussian shape. In Figure 7b we show the histogram of count rates of the same scintillator but including only left third of the horizontal scale. The variations of count rate in the selected time span include background fluctuation only and corresponding count rates are rather good described by Gaussian function as we can see from the goodness of fit positioned in the upper right corner of the Figure.

For calculation of the number of particles comprising TGE we use "Integral" mode of ADEI statistical package. Preceding from the calculated mean value of count rate this mode returns the total number of additional particles exceeding the mean (particles containing in the 2 peaks shown in Figure 7c).

In Figure 7c we can see an abrupt termination of the TGE possibly connected with nearby lightning. To uncover the correlation of particle fluxes and atmospheric discharges (one of the most important and yet unsolved problems of atmospheric physics) we use frames shown in Figure 8-10. In Figure 8 we show the one-minute time series measured by the 1-cm thick upper scintillator of STAND1 detector along with electrostatic field measurements by the electric mill EFM 100. Data from the electric mill allows as well estimation of the distance to lightning. We can see 2 nearby (distances 5.8 and 2 km) lightning flashes occurred during TGE.

The exact shapes of the TGE and electrostatic field disturbances are shown in Fig 9. From Figure 9 we can directly obtain the count rate decline due to lightning flashes occurred at 10:02:11and 10:05:13 (decline of 22% in 3 sec and 10% in 1 sec correspondingly).

To specify the lightning exact time and amplitude we need more detailed time series shown in Figure 10. The new fast DAQ electronics installed at Aragats in 2015 allows synchronization of particle fluxes and atmospheric discharges and exact determination of the atmospheric electric field disturbances (we show data only for the first lightning). The electrostatic field starts to rise at 10:02:11.488 from -16 kV/m until 10.02:11.638 to 48.1 kV/m. Thus the amplitude of the negative lightning was 64.1 kV/m achieved in 150 ms, field recovering took rather long ~48 sec.

Another important problem of the TGE atmospheric high-energy physics is research of the electron-gamma ray avalanches in the thundercloud. The energy spectra of electrons and gamma rays as measured by surface spectrometers can highly assist in this problem solving. To separate and estimate electron and gamma ray fluxes we use the CUBE detector consisted of two 20 cm thick plastic scintillators (upper N 7 and bottom N 8) fully covered by the 1 cm thick scintillators. This shielding provides "veto" for charged particles. Thus, 20-cm thick scintillators simultaneously register total flux (without veto) and neutral flux. Certainly, due to the non-zero efficiency of 1-cm plastic scintillators to miss charged particles (1-2%) and as well non-zero efficiency to detect neutral particles (2-3%) the flux separation is not absolute. However, according to techniques described in (Chilingarian, Mailyan and Vanyan, 2012) we can take into account scintillator efficiencies and calculate separate fluxes of TGE species. In the insert to Figure 11 we show the 1-minute count rates of upper and bottom 20-cm thick scintillators; in the body of Figure 11 we show the same time series, but in units of "number of standard deviations". The mean values of all four time series are calculated before the first peak.

ADEI allows export of data in as PNG pictures with controlled parameters (font size, size, number of ticks, resolution and other) and in the numerical form supporting most of standards. In table one we show the count rates from previous figure in numerical form. Also in last two columns, we show the ratio of 2 measurements for 2 scintillators. As we will, show below this ratio is sensitive to TGE amplitude in the case when most of TGE particles are gamma rays.

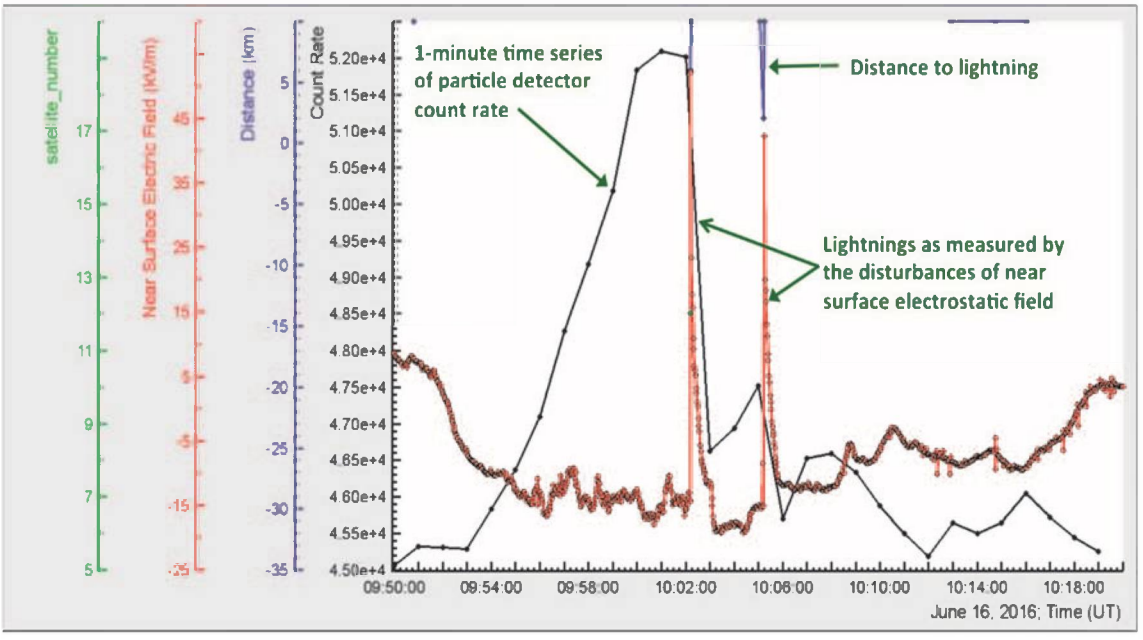

Figure 8. One minute time series of count rate of the 1-cm thick plastic scintillator belonging to STAND1 detector (upper, located nearby MAKET experimental hall) along with disturbances of the electrostatic field and distances to atmospheric discharges.

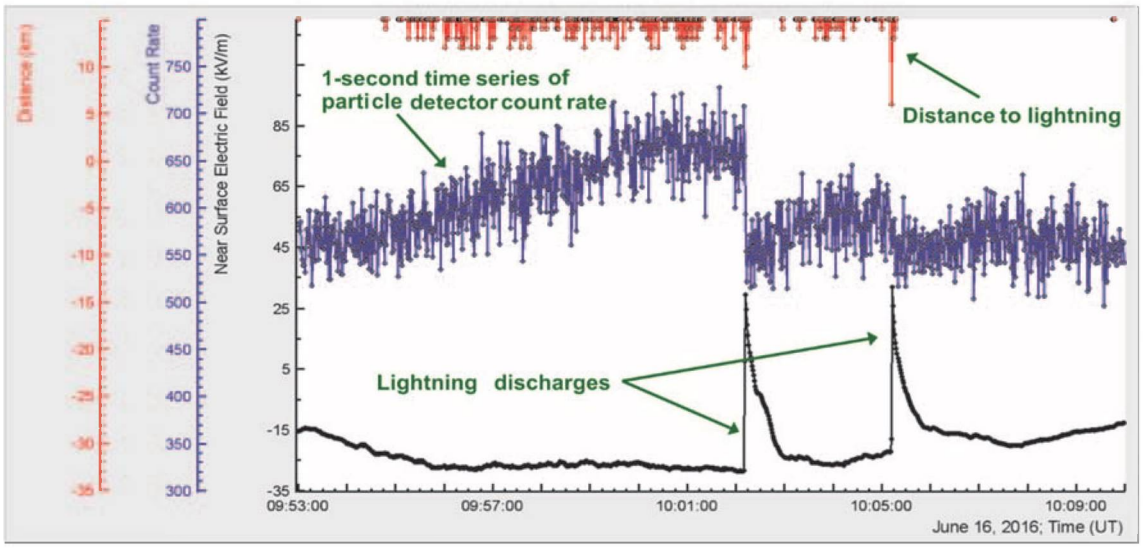

Figure 9. One second time series of count rate of the 3-cm thick plastic scintillator belonging to STAND1 detector (located nearby MAKET experimental hall) along with disturbances of the electrostatic field and distances to atmospheric discharges.

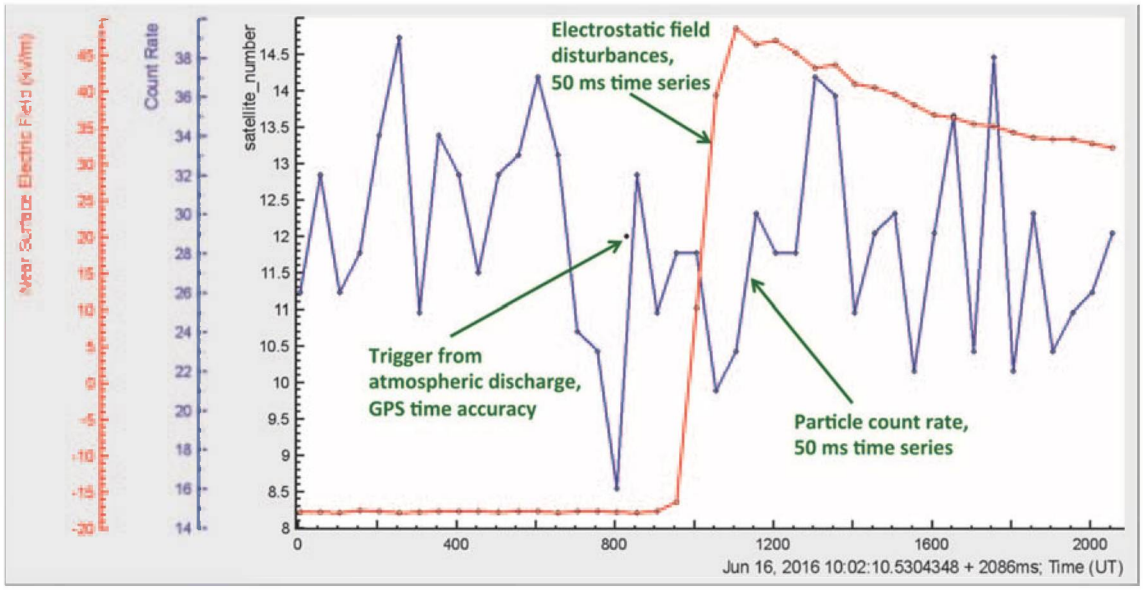

Figure 10. 50 ms time series of count rate of the 1-cm thick plastic scintillator belonging to STAND1 detector (upper, located nearby MAKET experimental hall) along with disturbances of the electrostatic field and distances to atmospheric discharges.

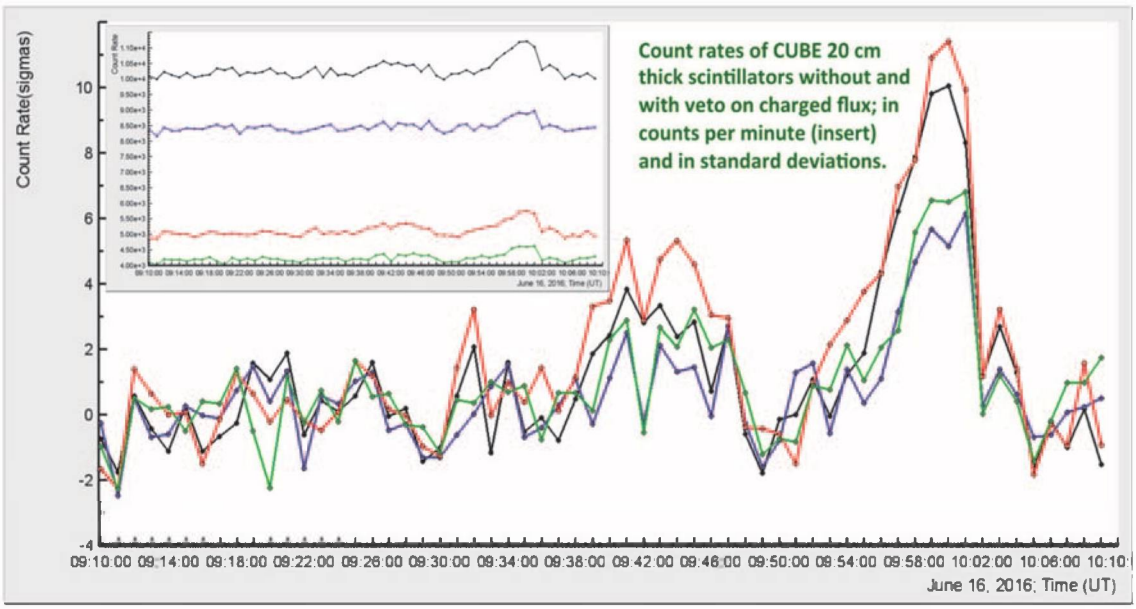

Figure 11. 1-minute time series of of 20-cm thick plastic scintillators of CUBE detector. In insert – natural units; main body – in number of standard deviations (Nσ).

In Table 2 we show the mean values of CUBE time series of count rates with and without veto at a fair weather and their ratio. The ratio is rather constant and differs from the ratio measured at 10:00-10:01 by 2.9σ (upper) and 3.7σ (bottom). Thus the ratio of count rates (with a veto to without veto) is a good indicator of TGE and its electron content.

In Table 3 we demonstrate the recovered by upper 20 cm scintillator intensities of electrons and gamma rays and fraction of electrons. Electrons attenuate in the air much faster than gamma rays. And sizable electron fraction in TGE is explained by the proximity of the cloud to earth's surface.

The NaI spectrometers and 60 cm thick plastic scintillators measure the energy release histograms from particles traversing detector. The radiation length of the NaI crystal is rather large ~5 and it is possible from the energy release histograms collected each minute recover the energy spectra of TGE as is shown in the Figure 12. The maximal energy of spectra >30 MeV is reached at 10:01 -10:02.

To relate the TGE fading due to declining of the electric field after lightning we measure energy release spectrum with 60 cm thick scintillators each 20 sec (Figure 13). The radiation length of 60 cm scintillator is ~ 1.6, thus we cannot recover energy spectra because a significant part of particle energy may not be released in the scintillator. However, the information from this scintillators allows us to notice that the high energy part of TGE disappeared after lightning occurred at 10:02:11. Thus lightning kills the avalanche process in the thundercloud. The low energy Compton scattered gamma rays are still registered but on a much lower scale.

Table 1. CUBE detector one minute time series. 2 inner 20 sm thick plastic scintillators with and without veto and their ratio.

16 June 2016	Upper scint. without veto	Bot. scint. without veto	Upper scint. with veto	Bot. scint. with veto	Upper with veto/without	Bottom with veto/without
9:54:00.0	10297	8522	5191	4310	0.504	0.506
9:55:00.0	10365	8428	5249	4239	0.506	0.503
9:56:00.0	10624	8495	5285	4305	0.498	0.507
9:57:00.0	10817	8683	5462	4341	0.505	0.5
9:58:00.0	10990	8825	5516	4543	0.502	0.515
9:59:00.0	11191	8916	5722	4608	0.511	0.517
10:00:00.0	**11215**	**8867**	**5755**	**4605**	**0.513**	**0.519**
10:01:00.0	11035	8961	5657	4626	0.513	0.516
10:02:00.0	10297	8420	5078	4169	0.493	0.489
10:03:00.0	10449	8522	5213	4248	0.499	0.498
10:04:00.0	10303	8451	5093	4195	0.494	0.496
10:05:00.0	10007	8331	4879	4072	0.488	0.489

Table 2. The mean values of 4 count rates measured by CUBE detector on fair weaher on 16 June 2016 and their ratio.

	Mean	σ	7 with veto/ 7without veto	8 with veto/8 without veto
Cube #7, 20cm	10168	103	0.493 +/- 0.007	0.497 +/- 0.006
Cube #8, 20cm	8389	87		
7 with veto	5013	62		
8 with veto	4172	61		

Table 3. The recovered electron and gamma ray fluxes and fraction of electrons in TGE flux on 16 June 2016.

Time	e intensity ($1/m^2min$)	γ intensity ($1/m^2min$)	e/ γ (%)
9:57-9:58	824	8896	9.3
9:58-9:59	1308	9928	13.1
9:59-10:0	1296	14048	9.2
10:00-10:01	1256	14716	8.5
10:01-10:02	920	12788	7.2
10:02-10:03	268	1248	21.5

In Figure 14 we demonstrate another option from ADEI statistical package. Some variables are "delayed" correlated, i.e. there is some inertia (several minutes or even several hours) when the influence of one of the variables becomes apparent on another one. For instance, we show in Figure 14c time series of outside temperature and count rate of NaI crystal located just under the roof of the SKL experimental hall. NaI crystal is sensitive to outside temperature and only after the metallic tits are heated enough they transfer heat to NaI crystals and count rate goes up. Certainty, the solar radiation is a key parameter influencing both temperature and then count rate. The simple correlation analysis is not applicable for such a dependences (Figure 14a). Therefore we include in ADEI stat package the delayed correlation option Figure 14c. From Figure 14b we can see that we need at least 3 hour of sun radiation till the particle detector "feel" the heat from the roof tilts.

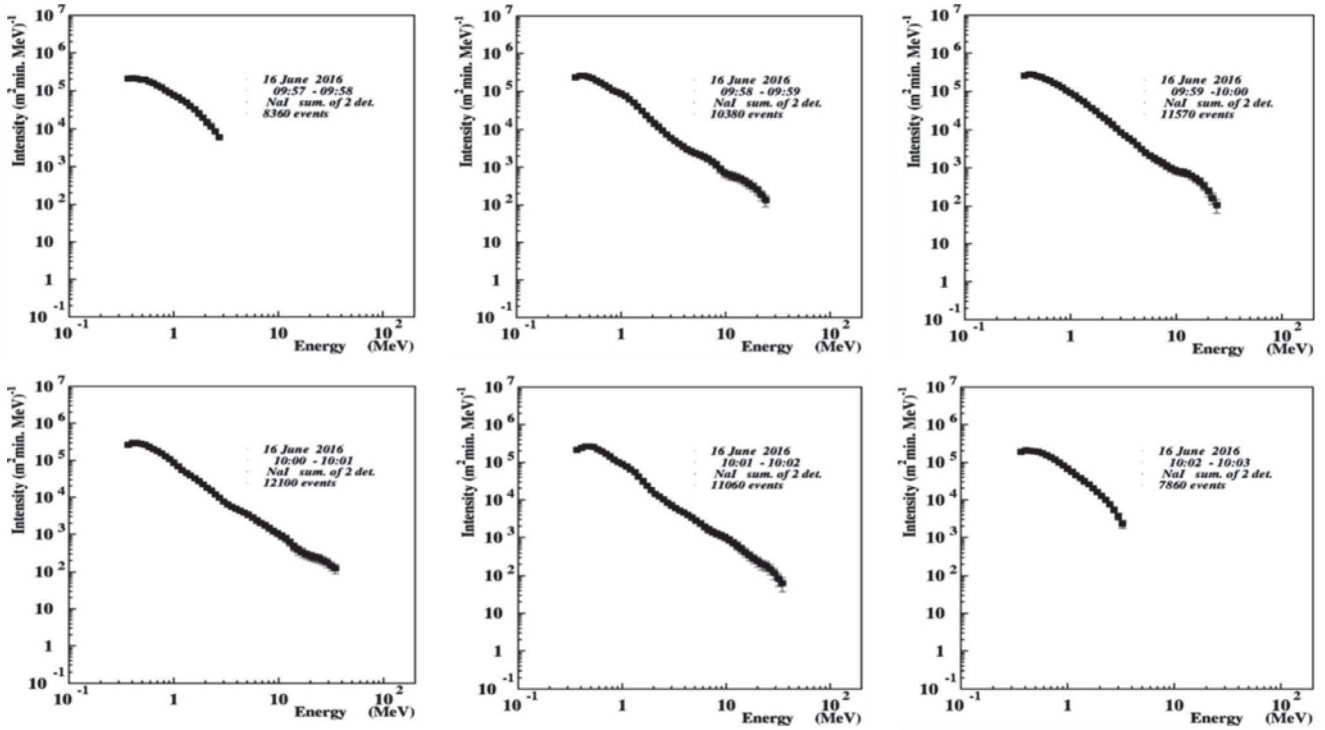

Figure 12. Energy spectra of TGE measured by the the network of NaI spectrometers.

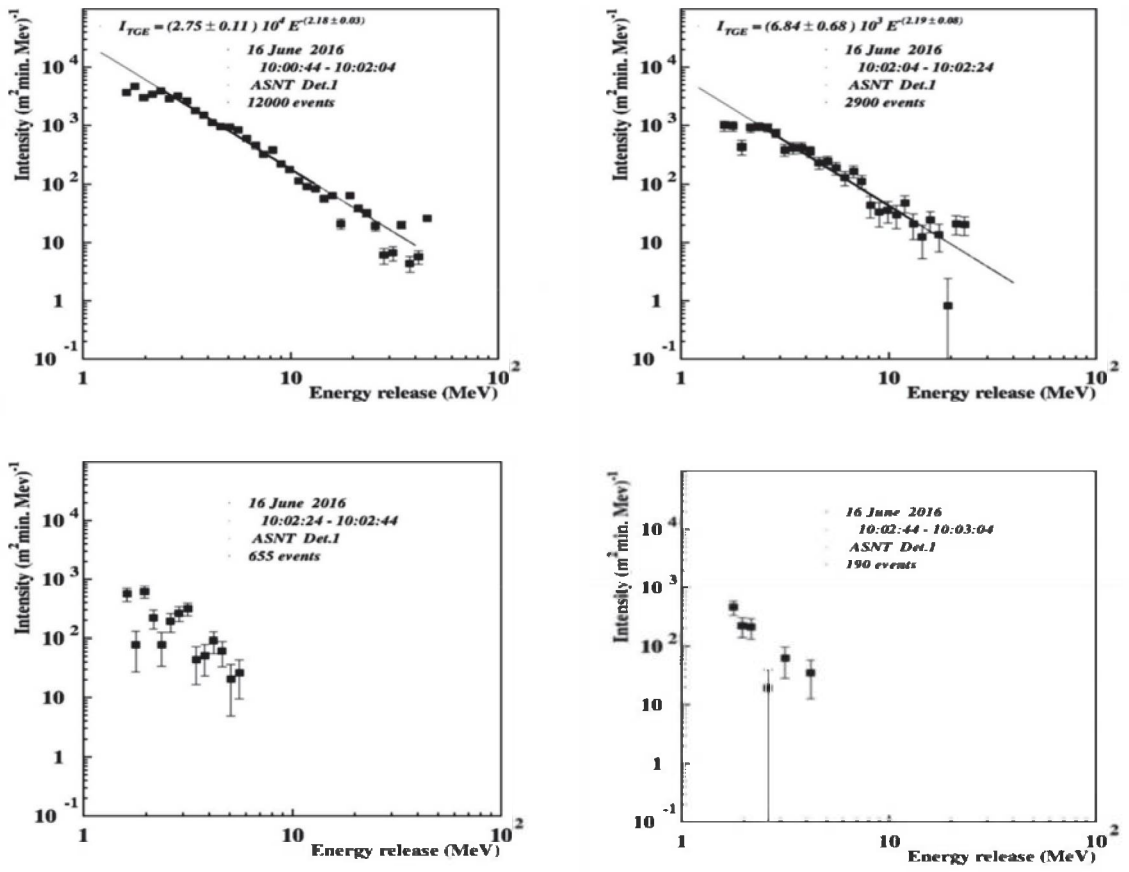

Figure 13. Energy release spectra measured by the the 60 cm thick plastic scintillator

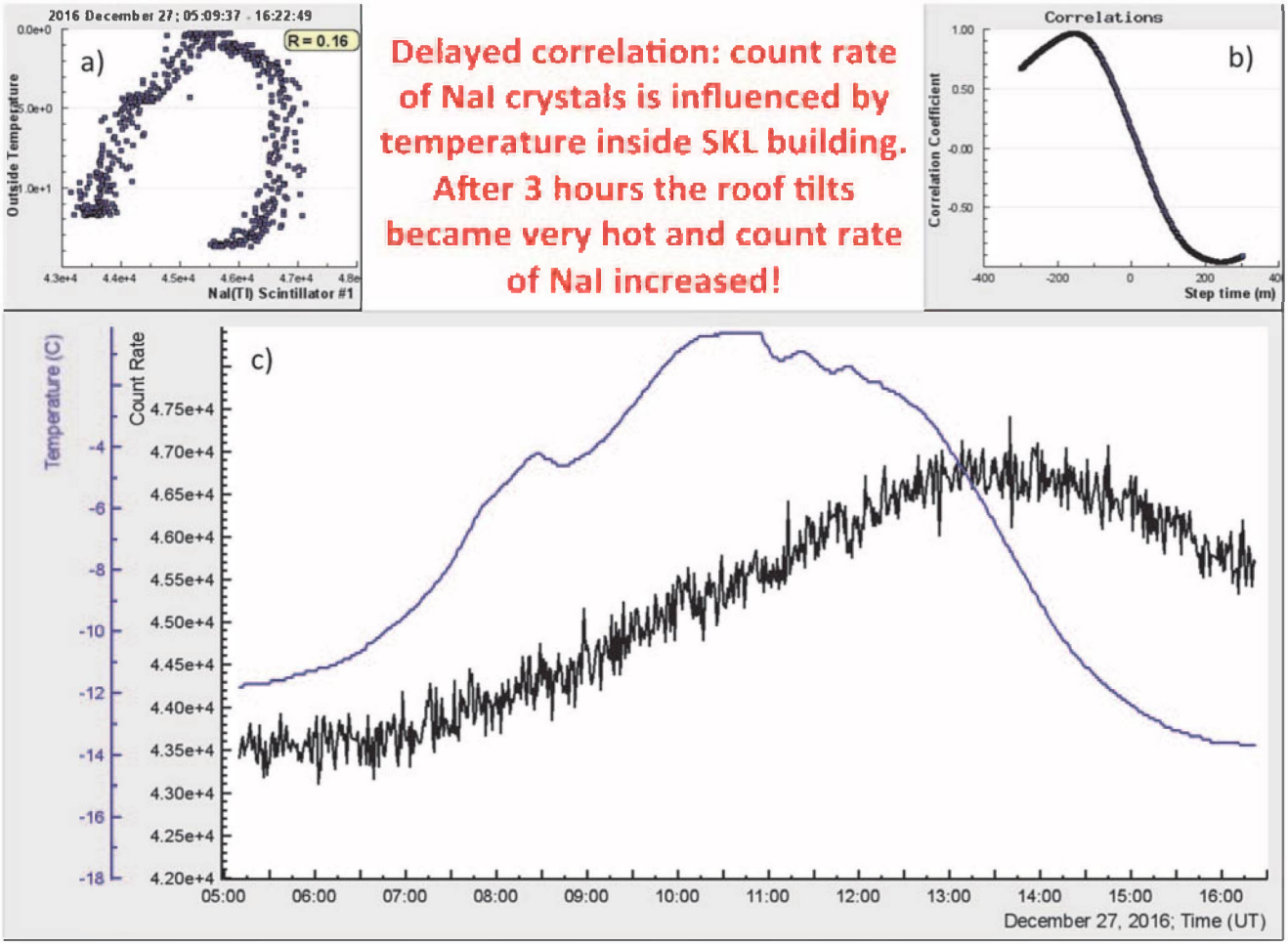

Figure 14. The 1-minute time series of outside temperature and NaI crystal count rate. In insert are shown results of simple correlation analysis and delayed analysis.

CONCLUSION

We describe in details how to apply ADEI procedures for analysis and physical inference in the atmospheric high-energy physics experiments. With the growing archives of the time series from the monitoring of the various cosmic ray fluxes and atmospheric electric field at ASEC, the need to establish a new type of infrastructures for using and comparing the data from numerous sources becomes more and more urgent. ADEI with new statistical modules meets this needs. To acquire the expected new knowledge, data samples from different domains are joining to make possible a multivariate correlation analysis. The developed methodology provides analysis tools and services to integrate a multitude of space and geophysical observations into a system that fully utilized the scientific potential of current and future geophysical observations. ADEI is used as well for the Space Weather and Solar physics research and we can present a set of ADEI layouts for physical inference in these domains. Physicists of Cosmic ray division prepare and publish in high-rank scientific journals near 20 articles heavily using ADEI platform in 2013 – 2016 (see the reference list). ADEI allows performing research projects very fast and comprehensive. ADEI tools make analytical work on the sophisticated problems rather easy; one can try and test many hypotheses very fast and come to definite conclusion allowing crosscheck and validation.

REFERENCE

S. Chilingaryan, A. Beglarian, A. Kopmann, and S. Vo¨cking, Advanced data extraction infrastructure: Web based system for management of time series data, J. Phys. Conf. Ser. 219, 042034 (2010).

Chilingarian A. and Reymers A., Investigations of the response of hybrid particle detectors for the Space Environmental Viewing and Analysis Network (SEVAN), Ann. Geophys, 26, (249- 257), 2008.

Chilingarian; Statistical study of the detection of solar protons of highest energies at 20 January 2005, Advances in Space Research 43 (2009), pp. 702-707.

Chilingaryan S., Chilingarian A., Danielyan V., et al; Advanced data acquisition system for SEVAN, Advances in Space Research 43 (2009) 717–720.

Chilingarian A., G. Hovsepyan, K. Arakelyan, et al; Space Environmental Viewing and Analysis Network (SEVAN), Earth, Moon and Planets: Volume 104, Issue 1 (2009), page 195.

Chilingarian A. and Bostanjyan N., Cosmic ray intensity increases detected by Aragats Space Environmental Center monitors during the 23rd solar activity cycle in correlation with geomagnetic storms, 2009, J. Geophys. Res., Vol. 114, No. A9, A09107

Chilingarian and N. Bostanjyan; On the relation of the Forbush decreases detected by ASEC monitors during the 23rd solar activity cycle with ICME parameters, Advances in Space Research, Volume 45, Issue 5, 1 March 2010, Pages 614-621

Mailyan, A. Chilingarian; Investigation of diurnal variations of cosmic ray fluxes measured with using ASEC and NMDB monitors, Advances in Space Research, 45, (2010) 1380–1387.

Chilingaryan S., Beglarian A., Kopmann A., and Vo¨cking S., J. Phys. Conf. Ser. 219, 042034 (2010).

Chilingarian A., A. Daryan, K. Arakelyan, A. Hovhannisyan, B. Mailyan, L. Melkumyan, G. Hovsepyan; Ground-based observations of thunderstorm-correlated fluxes of high-energy electrons, gamma rays, and neutrons (2010), Phys Rev D. 82.043009

Chilingarian A., Hovsepyan G., and Hovhannisyan A., Particle bursts from thunderclouds: Natural particle accelerators above our heads, Physical review D 83, 062001 (2011).

Chilingarian A., Karapetyan T., Calculation of the barometric coefficients at the start of the 24th solar activity cycle for particle detectors of Aragats Space Environmental Center, Advances in Space Research 47 (2011) 1140–1146.

Chilingarian A., Bostanjyan N., and Vanyan L., Neutron bursts associated with thunderstorms, PHYSICAL REVIEW D 85, 085017, 2012.

Chilingarian A., Bostanjyan N., and Vanyan L., Neutron bursts associated with thunderstorms, Physical Review D 85, 085017 (2012b).

Chilingarian A., Bostanjyan N., Karapetyan T., Vanyan L., Remarks on recent results on neutron production during thunderstorms, Physical Review D 86, 093017 (2012c).

Chilingarian, A. and Mkrtchyan, H., Role of the Lower Positive Charge Region (LPCR) in initiation of the Thunderstorm Ground Enhancements (TGEs), Physical Review D 86, 072003 (2012d).

Chilingarian A., Mailyan B., Recovering of the TGE electron and gamma ray energy spectra, Journal of Physics: Conference Series 409 (2013) 012214.

A Chilingarian, N Bostanjyan, T Karapetyan, On the possibility of location of radiation-emitting region in thundercloud, Journal of Physics: Conference Series 409 (2013) 012217.

Avakyan K., Arakelyan K., Chilingarian A., et al., NaI Detector Network at Aragats, Journal of Physics: Conference Series 409 (2013) 012218.

Chilingarian A., Bostanjyan N., Karapetyan T.,Vanyan L., Neutron production during thunderstorms, Journal of Physics: Conference Series 409 (2013) 012216.

Chilingarian A., Thunderstorm Ground Enhancements (TGEs) - New High- Energy Phenomenon Originated in the Terrestrial Atmosphere, Journal of Physics: Conference Series 409 (2013) 012019 Chilingarian A., Hovsepyan G., Extensive Cloud Showers (ECS) – New High-Energy Phenomena Resulting from the Thunderstorm Atmospheres , Journal of Physics: Conference Series 409 (2013) 012221.

Chilingarian A., Vanyan L., Simulations of the secondary cosmic ray propagation in the thunderstorm atmospheres resulting in the Thunderstorm ground enhancements (TGEs), Journal of Physics: Conference Series 409 (2013) 012215.

Chilingarian A. and Mkrtchyan H., Lower positive charge region (LPCR) and its influence on initiation of Thunderstorm ground enhancements (TGEs) and cloud-to-ground (CG-) and intracloud (IC-) lightning occurrences, Journal of Physics: Conference Series 409 (2013) 012219

Chilingarian A., Karapetan T., Melkumyan L., Statistical analysis of the Thunderstorm Ground Enhancements (TGEs) detected on Mt. Aragats. J. Adv. Space Res., 52, 1178 (2013),

Chilingarian A., Mailyan B., Vanyan L., Observation of Thunderstorm Ground Enhancements with intense fluxes of high-energy electrons, Astropart. Phys., 48, 1 (2013)

Chilingarian A., Hovsepyan G., and Kozliner L., Thunderstorm ground enhancements: Gamma ray differential energy spectra, Physical Review D 88, 073001 (2013).

Chilingarian, A., Exploring High-Energy Phenomena in Earth's Atmosphere, Eos Trans. AGU, 94(50), 488 (2013).

Chilingarian A., Thunderstorm Ground Enhancements - model and relation to lightning flashes, Journal of Atmospheric and Solar-Terrestrial Physics, 107, 68-76, 2014.

Chilingarian A., Hovsepyan G., Vanyan L., On the origin of the particle fluxes from the thunderclouds: energy spectra analysis, EPL, 106 (2014) 59001

Chilingarian A., Exploring the Origin of High-Energy Particle Beams in the Atmosphere, Eos, Vol. 95, No. 46, 18 November 2014

Chilingarian A., Chilingaryan S., Hovsepyan G., Calibration of particle detectors for secondary cosmic rays using gamma-ray beams from thunderclouds, Astroparticle Physics 69 (2015) 37–43

Chilingarian A., Hovsepyan G., Khanikyanc Y., Reymers A. and Soghomonyan S., Lightning origination and thunderstorm ground enhancements terminated by the lightning flash, EPL, 110 (2015) 49001

Chilingarian, A., Chilingaryan S., and Reymers A., Atmospheric discharges and particle fluxes, J. Geophys. Res. Space Physics, 120, 5845–5853 (2015),doi:10.1002/2015JA021259.

Chilingarian A., Hovsepyan G., and Mantasakanyan E., Mount Aragats as a stable electron accelerator for atmospheric High-energy physics research, Phys. Rev. D: Part. Fields, 93, 052006 (2016).

Chilingarian, A. Where does lightning come from?, Eos, 97 (2016), doi:10.1029/2016EO050097.

Chilingarian A., Hovsepyan G., Kozliner L., Extensive Air Showers, Lightning, and Thunderstorm Ground Enhancements, Astroparticle Physics 82 (2016) 21–35.

Drozdov, A. Y., A. Grigoriev, and Y. Malyshkin (2012), Assessment of thunderstorm neutron radiation environment at altitudes of aviation flights, J. Geophys. Res., doi:10.1029/2012JA018302, in press.

Hovhannisyan A., A. Chilingarian; Median filtering algorithms for multichannel detectors, Advances in Space Research 47 (2011) 1544–1557